НАУЧНО-ТЕХНИЧЕСКИЙ ВЕСТНИК ИНФОРМАЦИОННЫХ ТЕХНОЛОГИЙ, МЕХАНИКИ И ОПТИКИ
июль–август 2025 Том 25 № 4 http://ntv.ifmo.ru/
SCIENTIFIC AND TECHNICAL JOURNAL OF INFORMATION TECHNOLOGIES, MECHANICS AND OPTICS
Jule–August 2025 Vol. 25 No 4 http://ntv.ifmo.ru/en/
ISSN 2226-1494 (print) ISSN 2500-0373 (online)

doi: 10.17586/2226-1494-2025-25-4-617-625

Characterization of Ar:N_2 plasma mixture with optical emission spectroscopy during deposition of NbN coating

Harakat Mohsin Roomy[1]✉, Mohammed K. Khalaf[2], Mohammed G. Hammed[3]

[1] Ministry of Education, Baghdad, 10011, Iraq
[2] Ministry of Science and Technology, Baghdad, 10011, Iraq
[3] University of Anbar, Ramadi, 31011, Iraq

[1] hrkatm37@gmail.com✉, https://orcid.org/0000-0002-7919-4463
[2] mohammed.k.khalaf@src.edu.iq, https://orcid.org/0000-0001-5688-6304
[3] Sc.moh72_gh@uoanbar.edu.iq, https://orcid.org/0000-0002-0226-702X

Abstract

The combination of optical emission spectroscopy with models of plasma light emission represents a non-intrusive and adaptable approach for determining plasma characteristics. This study aimed to investigate the plasma electron temperature, electron density, and other parameters of plasma within context DC magnetron sputtering, under a various experimental condition, in the existence of a Niobium target and an Argon:Nitrogen gas mixture. To evaluate electron temperature and electron density, optical emission spectroscopy was employed at a range of discharge voltages (400–800 V) and gas pressures (0.04–3.3 mbar). The measurements were taken during the deposition of a Niobium nitride coating with in magnetron sputtering setup, maintaining a gap distance of 0.06 m and a total flow rate of 40 Standard Cubic Centimeters per Minute. The temperature of electron was assessed using Boltzmann plot strategy with several ion lines Ar^+ lines, while density of electron was determined from the intensity ratio of atomic to ionic lines using Saha-Boltzmann equation. The results demonstrate that, for the plasma under investigation, an increase in the applied voltage lead to an elevation of temperature of electron, while an increase in the working pressure results in a reduction in the temperature of electron. Conversely, the density of electron decreases with the increasing applied voltage and increases with rising working pressure. Additionally, the findings indicate that the introduction of a modest quantity of nitrogen gas into the discharge source resulted in improved electrical characterization of the glowing discharge plasma during the Niobium nitride coating deposition process.

Keywords

optical emission spectroscopy, parameters of plasma, glow discharges, electron temperature, electron density

Acknowledgements

Our thanks and appreciation to the laboratories of the University of Baghdad and the Ministry of Science and Technology for completing the requirements of this study.

For citation: Roomy H.M., Khalaf M.K., Hammed M.G. Characterization of Ar:N_2 plasma mixture with optical emission spectroscopy during deposition of NbN coating. *Scientific and Technical Journal of Information Technologies, Mechanics and Optics*, 2025, vol. 25, no. 4, pp. 617–625. doi: 10.17586/2226-1494-2025-25-4-617-625

УДК 621.793.16

Характеризация плазменной смеси Ar:N_2 с помощью оптической эмиссионной спектроскопии при магнетронном осаждении покрытия NbN

Харакат Мохсин Руми[1]✉, Мохаммед К. Халаф[2], Мохаммед Г. Хаммед[3]

[1] Министерство образования, Багдад, 10011, Ирак
[2] Министерство науки и технологий, 10011, Ирак
[3] Университет Анбар, Анбар, 31011, Ирак

[1] hrkatm37@gmail.com✉, https://orcid.org/0000-0002-7919-4463
[2] mohammed.k.khalaf@src.edu.iq, https://orcid.org/0000-0001-5688-6304
[3] Sc.moh72_gh@uoanbar.edu.iq, https://orcid.org/0000-0002-0226-702X

Аннотация
Сочетание оптической эмиссионной спектроскопии с моделированием плазменного светового излучения представляет собой неинтрузивный и адаптируемый подход к определению характеристик плазмы. Целью данного исследования было изучение температуры электронов плазмы, электронной плотности и других параметров плазмы при магнетронном распылении на постоянном токе в различных экспериментальных условиях в присутствии ниобиевой мишени и газовой смеси аргон-азот (Ar:N_2). Для оценки температуры и электронной плотности использовалась оптическая эмиссионная спектроскопия в диапазоне напряжений разряда 400–800 В и давлений газа 0,04–3,3 мбар. Измерения проводились во время осаждения покрытия из нитрида ниобия (NbN) методом магнетронного распыления при поддержке расстояния между зазорами 0,06 м и общей скорости потока 40 стандартных кубических сантиметров в минуту. Температура электронов оценивалась путем построения графика Больцмана с несколькими ионными линиями Ar^+, а плотность электронов определялась из отношения интенсивностей атомных и ионных линий с использованием уравнения Саха–Больцмана. Результаты исследований показали, что увеличение приложенного напряжения приводит к повышению температуры электронов, в то время как увеличение рабочего давления приводит к снижению температуры электронов. Наоборот, плотность электронов уменьшается с увеличением приложенного напряжения и увеличивается с ростом рабочего давления. Показано, что введение небольшого количества N_2 в источник разряда во время процесса осаждения NbN приводит к улучшению электрических характеристик плазмы тлеющего разряда.

Ключевые слова
оптическая эмиссионная спектроскопия, параметры плазмы, тлеющие разряды, электронная температура, электронная плотность

Благодарности
Авторы выражают благодарность и признательность лабораториям Багдадского университета и Министерству науки и технологий Республики Ирак за выполнение требований данного исследования.

Ссылка для цитирования: Руми Х.М., Халаф М.К., Хаммед М.Г. Характеризация плазменной смеси Ar:N_2 с помощью оптической эмиссионной спектроскопии при магнетронном осаждении покрытия NbN // Научно-технический вестник информационных технологий, механики и оптики. 2025. Т. 25, № 4. С. 617–625 (на англ. яз.). doi: 10.17586/2226-1494-2025-25-4-617-625

Introduction

Low-temperature plasmas are systems that are significantly out of equilibrium, producing distinctive physical and chemical conditions by means of free electrons in low-temperature gas. The unique environment allows for the precise treatment of temperature-sensitive materials with atomic and molecular accuracy. Plasma technologies are a valuable resource for numerous high-end industries [1–3]. Electron temperature (T_e) is typically used to describe plasma because electrons, being much smaller and lighter than ions, achieve thermal equilibrium more quickly. This means their energy distribution stabilizes faster than that of the much heavier ions [2]. T_e determines many properties of the plasma, including electrical conductivity, light emission, and how it interacts with magnetic and electric fields. This makes it a vital parameter in various applications, from industrial plasma processes to astrophysical studies [4]. The nitrogen molecules (N_2) presented in Argon:Nitrogen (Ar:N_2) admixture plasma undergo a series of atomic transformations resulting in the formation of various atomic nitrogen species. These species possess a range of industrial applications, including thin layer deposition, surface chemistry, nitride thin layers, material modification, etching, surface sterilization, and the alteration of the surface properties of different materials [5–7]. Spectral diagnostics of glow discharge plasma involve detailed analyses of the radiation it emits or absorbs. By examining emission strength, absorption features, and the broadening or shifting of spectral lines, scientists can deduce critical plasma properties. These methods enable precise control and understanding of plasma behavior, supporting advancements in research and industrial applications [8]. The Optical Emission Spectroscopy (OES) is utilized to monitor the plasma and assurance that has arrived at consistent state rapidly after start. The evolution of a line emission over time is used to determine plasma stability [9, 10]. Contingent upon the gas creation and plasma properties, all plasma produces radiation. It is mostly known that when a molecular gas is added to a rare gas, the discharge characteristics can change dramatically, affecting the type and intensity of radiation produced [11]. The magnitude besides the pattern of these changes is influenced by the conditions of discharge: the type of rare gas, the type besides the degree of mixing, and the gas pressure, etc. The Ar:N_2 is considered to be one of the most commonly used mixtures in discharge investigations as a gas mixture [12]. Because of its potential for technological applications, for decades, scientists have examined low pressure plasma in N_2 glow discharges. The active species generated in these processes are crucial for a variety of applications, including plasma-assisted ignition, biological sterilization and heating, combustion, surface treatment, and the destruction of hazardous chemicals and pollutants [11, 13]. In the context of plasma physics, low-pressure discharge operating conditions are frequently delineated in terms of T_e and electron density (n_e). These parameters are of paramount importance for comprehending the behavior and properties of the plasma. OES is a widely utilized non-meddlesome diagnostic tool for analyzing plasmas [14]. The method operates by detecting the light emitted from excited atoms and molecules as they return to lower energy states. The intensity and wavelengths of this emitted light provide essential data to model and optimize plasma processes by offering insights into each T_e and n_e which are fundamental in determining the energy distribution and behavior of the plasma [15]. By exposing a sample to Ar:N_2 plasma, it is possible to achieve

a balance between nitriding and sputtering processes, thereby forming a controlled and effective nitride layer. An understanding of, and ability to manipulate, ion flux and plasma parameters is essential for the tailoring of surface properties to meet specific application requirements [16]. The barraging particle sort and active energy, as well as the sort and surface state of the substance to be utilized, are exceedingly significant components in deciding the sputtering rate [17]. A spectroscopic strategy can gauge the electron temperature in various ways; Boltzmann's plot is the best regularly involved spectroscopic demonstrative methodology for deciding the T_e in the research center plasma [18], which ensures greater precision by assuming Boltzmann distribution for the population of emitting levels. The intensities of numerous spectral lines with varied threshold excitation energies are used to determine the T_e in this method [19]. The T_e and n_e represent the most fundamental characteristics of plasmas, exerting a significant influence on the operational and maintenance dynamics of gas discharges. The experimental results of a parametric investigation of atmospheric plasma characteristics are presented in this work. The atomic emission line intensities were employed to calculate plasma characteristics, including temperature, intensity of electron, and other plasma parameters in the presence of a Niobium target (Nb) and an Ar:N_2 gas mixture. The study employed the OES method, whereby the discharge conditions were varied. These included the applied voltage and operational pressure in an Ar:N_2 plasma which was generated using a Nb target and its deposited Niobium nitride (NbN) coating.

Theoretical approach

Numerous spectroscopic methods can be used to calculate the T_e, but Boltzmann's plot is the most widely used approach in laboratory plasmas due to its higher accuracy. This methodology defines the T_e by using the intensities of several spectral lines with different threshold excitation energies.

This can be accomplished by making the assumption that the population of emitting levels is distributed according to Boltzmann's law. The T_e is gained from the slope of the Boltzmann's plot utilizing several of argon ion (Ar^+) spectral lines that share a common lower level. This relationship enables the Boltzmann plot method to evaluate the T_e [20, 21]:

$$\ln\left(\frac{\lambda I}{Ag_u}\right) = -\frac{E_u}{K_B T_e} + C,$$

where I is the relative intensity of the emitted line; λ is the wavelength; the upper-level statistical weight, signified by the symbol g_u, can be intended using the total angular momentum quantum number (J), according to the association ($g = 2J + 1$); A represents the transition probability which quantifies the probability that an atom in an upper level state will randomly emit a photon and subsequently de-excite to a lower level state with a frequency of once every second; K_B is the Boltzmann constant ($1.38 \cdot 10^{-23}$ J/K); T_e is the temperature of electron in K; E_u is defined as energy originating from a higher level of existence; C is a constant; and $\left(\frac{\lambda I}{Ag_u}\right)$ is the relative intensity of the emitted line. The verse energies of the higher level of E_u are linearly related and characterized by a slope of $(1/T_e)$. The n_e can be computed using the Saha-Boltzmann equation, which is written as follows, from the emission of singly charged ion (ionic) and neutral particle (atomic) spectral lines in the plasma [22]:

$$n_e = 6.04 \cdot 10^{21} (T_e)^{3/2} \frac{I^a \lambda^a g^i A^i}{I^i \lambda^i g^a A^a} \exp \frac{E^a - E_{ion} - E^i}{K_B T_e},$$

where the higher indices (a) and (i) for parameters stand for the neutral particle and singly charged ion, respectively; the ionization energy of the neutral particle is well-established and is denoted by the symbol E_{ion}. The atomic spectral database of the National Institute of Standards and Technology (NIST) contains the values of E_u, A, E_{ion}, and g_u. Debye shielding ensures that plasmas maintain their quasi-neutrality by limiting the spatial extent of electric fields through the rearrangement of charges. The Debye length (λ_D) provides a measure of the characteristic scale over which this shielding occurs. The mathematical expression for the λ_D is [23]:

$$\lambda_D = \sqrt{\frac{\varepsilon_\circ K_B T_e}{e^2 n_e}},$$

where e is the electron charge; $\varepsilon_\circ$ is the electric constant density. The plasma parameter (N_D) quantifies the total amount of particles contained within the Debye sphere. The shielding effect is only possible if there are enough electrons in the Debye sphere. Given the exponential decay of the potential, it can be posited that the shielding is attributable to the electrons within the Debye sphere the quantity of which is denoted by:

$$N_D = \frac{4\pi}{3} n_e \lambda_D^3.$$

The typical time scale and response of a plasma to external fields are determined by the plasma frequency. When plasma particles are moved from their equilibrium positions, a space charge field is created to restore the plasma neutrality by pulling the particles back to their original positions. These oscillations occur at a frequency known as the plasma frequency of the electron (W_{pe}) which can be expressed as [24]:

$$W_{pe} = \left(\frac{e^2 n_e}{\varepsilon_\circ m}\right)^{1/2},$$

where m is the mass of electron.

Experimental Details

Plasma system

Fig. 1 shows a picture of the principle experimental part used in this search. The an-homemade Magnetron Sputtering Plasmas procedure is usually used for materials processing which has been manufactured and based on the

following principles components. One of these work tools in the plasma chamber: cylindrical vacuum chamber from stainless steel by diameter and length of 30 cm and 40 cm, respectively. The chamber consists of two electrodes, there may be a glow discharge between these electrodes, one of the electrodes is movable and the second one is fixed electrode (denoted as cathode (magnetron)). To prevent power dissipation, the magnetron was cooled by water circulation. Additionally, the chamber was equipped with a single side window and four feedthroughs for vacuum. These included feedthroughs are: high voltage, electrical, cathode cooling, and gas supply. The vacuum system consisted of a rotary pump and a dry scroll pump. The range of this setup resulted in a vacuum of $1.33 \cdot 10^{-6}$ mbar. The plasma system consists of two distinct components: the first of which is the gas supply system, including Ar, N_2, and a pressure control system that serves to stabilize the pressures of the plasma within the chamber at a predefined value. The flow pressure of the gas mixture delivered to the plasma chamber was regulated by flow meters and a needle valve. To discharge foundation gases, the chamber was evacuated to around $1 \cdot 10^{-5}$ mbar. The cathode confronted the anode with 0.06 m spacing, anode circle (glass substrates) and cathode (Nb target). A high-purity (99.9 %) Nb target was employed as a disc with a diameter of 5 cm and a thickness of 3 mm. The operational gas Ar:N_2 gaseous mixture is considered, and the N_2 contribution in the Ar:N_2 mixture is (20, 30, 50 %), but the total flow rate was kept at 40 Standard Cubic Centimeters per Minute. The emission spectra at (200–900 nm) are recorded. An applied voltage was utilized running between 400 to 800 V and working pressure of Ar:N_2 going between $4 \cdot 10^{-2}$ and $3.3 \cdot 10^{-1}$ mbar. Plasma induced OES is conducted via a computer-controlled system comprising a spectrophotometer and an optical cable linked to a collecting optical lens. This lens is positioned towards the quartz window chamber. A spectrometer with a spectral resolution Full Width at Half Maximum (FWHM) of 2.5 nm is employed to collect radiation generated by the plasma. The spectrometer is a Surwit technology device V2100 which is capable of measuring ultraviolet and near-infrared radiation.

Results and Discussion

Six different spectral lines (750.3869, 751.4652, 763.5106, 772.3761, 811.5311, and 842.4648 nm) are selected to measure the plasma properties of argon plasma. The essential data of Ar^+ spectral lines (λ, A, E_u, and g) are presented in Table 1 which can be gained from NIST 2014, while the relative intensity taken from OES.

Fig. 2, *a* displays the contrasts of the net discharges of the different outflow lines emanating from the Ar:N_2(70:30) combination gas plasma species as a function of operating

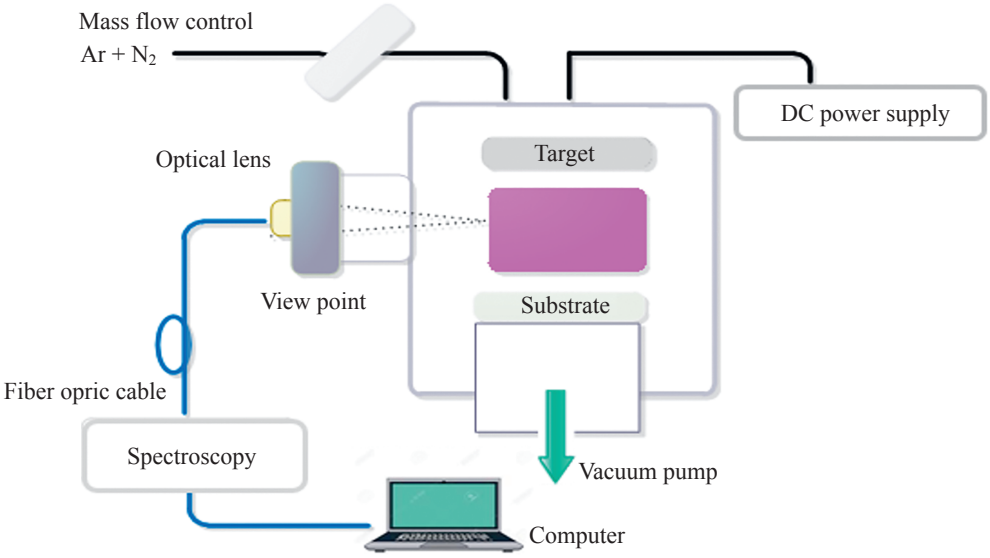

Fig. 1. Schematic diagram of the experimental system

Table 1. Spectroscopic data (λ, E, A, and g) besides fitting parameters corresponding to the selected Ar lines emitted by the Ar:N_2-rich plasma employed in this study

Ion	Wavelength λ, nm	Upper energy level E, eV	Transition probability $A \times 10^7$ s^{-1}	Statistical weight g
Ar^+	750.3869	13.47988670	4.45	1
Ar^+	751.4652	13.27303799	4.02	1
Ar^+	763.5106	13.17177759	2.45	5
Ar^+	772.3761	13.15314370	0.51	3
Ar^+	811.5311	13.07571560	3.31	7
Ar^+	842.4648	13.09487245	2.15	5

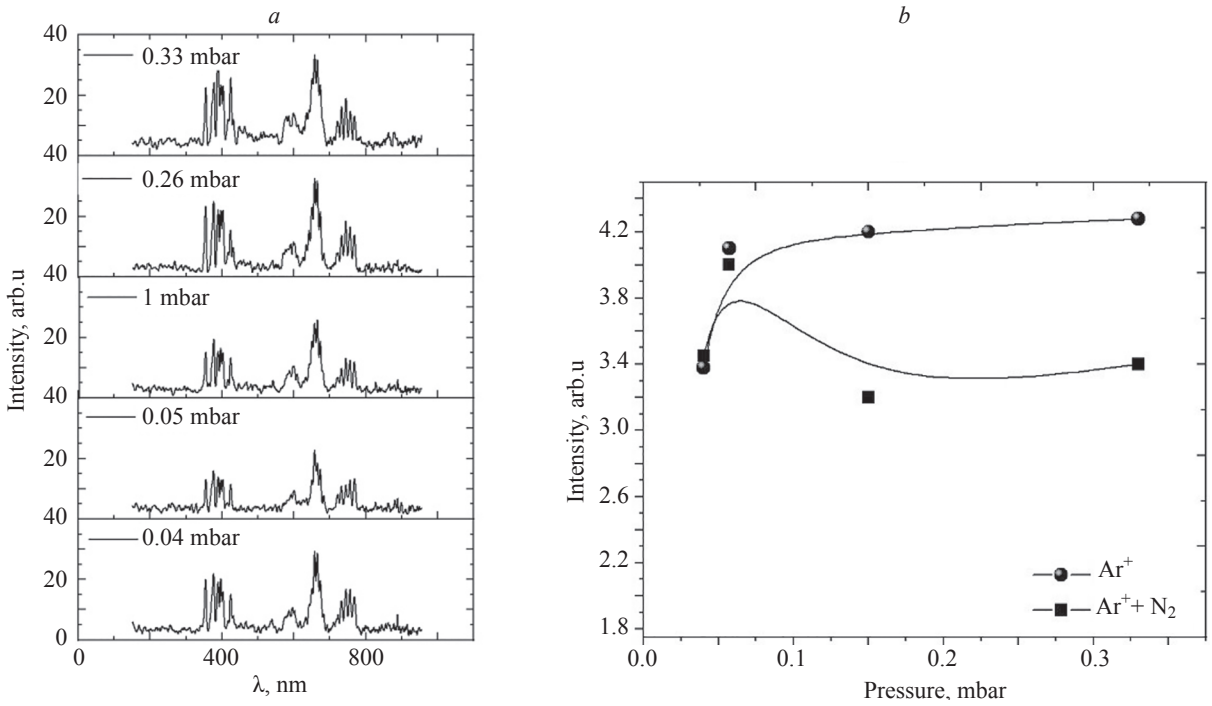

Fig. 2. Emission spectrum in Ar:N_2 mixture gas (*a*). Intensity of Ar^+ and Ar + N_2 as a function of the pressure (*b*)

pressure. When using pure argon as the plasma gas, the powers of the Ar^+ lines increase as the working pressure increases. However, when compared to the mixed Ar:N_2 plasma, there is a notable contrast. The Ar^+ and nitrogen spectral lines in the Ar:N_2 combination show weaker intensities than those observed in the pure argon plasma as shown Fig. 2, *b*. This reduced intensity in the mixed plasma suggests that the presence of nitrogen affects the overall energy distribution and excitation dynamics within the plasma. Nitrogen likely alters the excitation balance, either through quenching effects or through energy transfer processes that divert energy away from Ar emissions. This could be attributed to the complex interplay between argon and nitrogen species, influencing the energy states and radiative transitions in the plasma. As a sample exposed to an Ar:N_2 plasma interacts with active nitrogen species, it is likely to become rapidly coated with nitride layers. These surface layers can further modify the surface chemistry and sputtering dynamics, forming a barrier that affects further sputtering and alters the emission characteristics observed in the plasma. This behavior contributes to the striking contrast between the sputtering rates and resulting plasma emission characteristics of pure Ar and mixed Ar:N_2 environments.

Fig. 3, *a* depicts the comparative analysis of net discharge emissions from diverse output lines emanating from the Ar:N_2 (70:30) combination gas plasma, as a function of applied voltage. The figure elucidates the influence of voltage alterations on the emission intensity and characteristics of plasma species. As the applied voltage increases, the energy supplied to the plasma enhances the excitation and ionization processes. In the context of pure argon plasma, this results in a marked increase in the emission intensities of Ar^+ spectral lines as displayed in Fig. 3, *b*. The increase in energy leads to more frequent collisions between electrons and argon atoms, promoting higher excitation states and stronger photon emissions. In the Ar:N_2 mixture, however, the behavior shows distinctive features compared to pure argon. The presence of nitrogen introduces competing processes that can alter the energy distribution among the species. While the Ar^+ emission lines in the combination gas may still increase with applied voltage, their growth rate is typically less pronounced compared to pure argon. This is because the excitation and ionization processes are shared between argon and nitrogen. Nitrogen ability to ionize more readily and form active species such as (ionized nitrogen molecules) and other nitrogen radicals results in a redistribution of energy, which can suppress the peak intensities of Ar emissions as the applied voltage is increased.

X-Ray Diffraction Analysis

As illustrated in Fig. 4, the X-Ray Diffraction (XRD) patterns of NbN thin layers deposited at varying N_2 ratios (20 %, 30 %, and 50 %) in Ar:N_2 gas mixtures were examined. It was observed that the peak intensity (200) at $2\theta = 23.15°$ for the NbN nanoparticles coating deposited at 30 % was higher than that of the coating deposited at 20 % and 50 %. This diffraction angle corresponds to twice the angle (θ) between the incident X-ray beam and the diffracting crystal planes, and expressed in degrees. This finding indicates that the structure of NbN thin layers has a cubic construction, which is in excellent agreement with the International Centre for Diffraction Data card no. 75-0592. The absence of additional peaks detected indicates that the high-purity phase was synthesized in the absence of impurities. As the Ar:N_2 ratio changes from 80:20 to 70:30, the XRD analysis shows a noticeable rise in FWHM from 0.2500° to 0.5500°. A notable decrease in crystallite size from 32.4 nm to 14.8 nm is linked to this widening. The higher nitrogen content probably causes more lattice strain

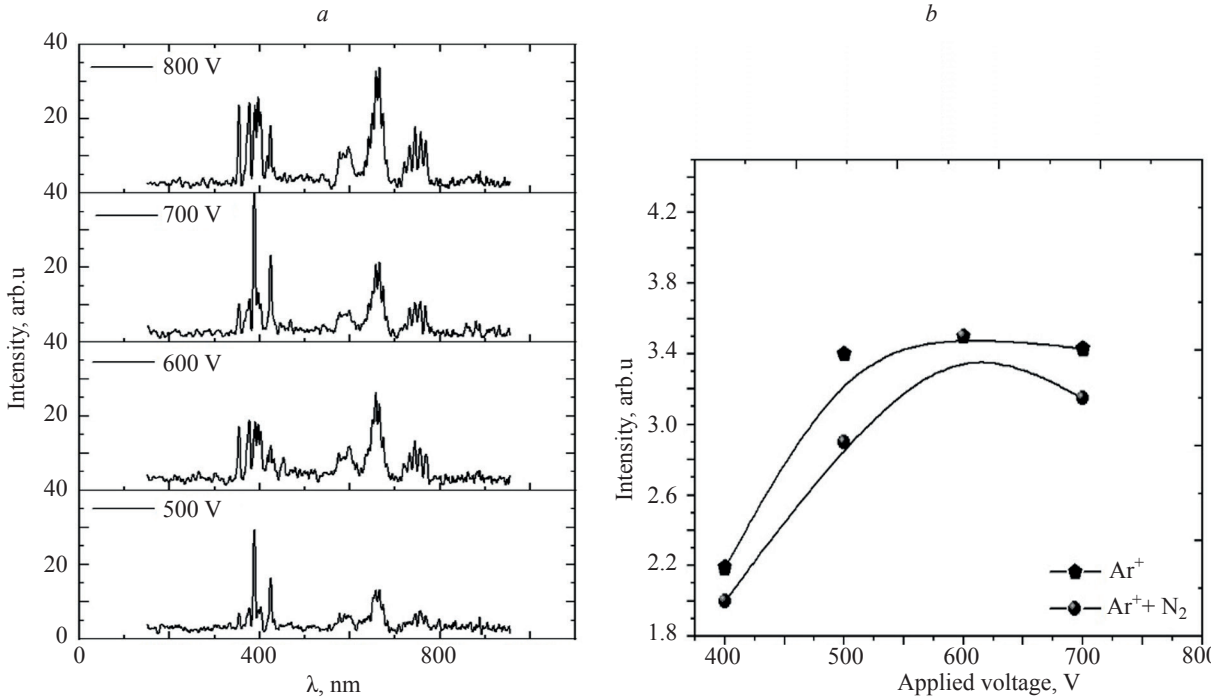

Fig. 3. Emission spectrum in Ar:N_2 mixture gas (*a*). Intensity of Ar^+ and $Ar^+ + N_2$ as a function of applied voltage (*b*)

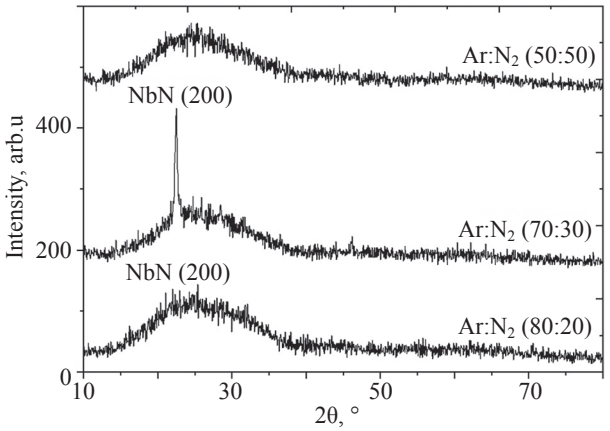

Fig. 4. XRD patterns for the NbN coating at different gas ratio

and disorder, which hinders the formation of crystallites and lowers the structural quality. The Miller indices (h, k, l) used to indicate the orientation of crystallographic planes in a crystal lattice, are denoted by the notation (hkl) in Table 2. The plane labeled (200) represents a set of planes that intercept the crystallographic axes in a specific. The results of XRD analysis are summarized in Table 2.

Plasma parameter evaluation

This relationship between T_e and pressure is critical for optimizing deposition parameters to achieve the desired NbN thin film characteristics, such as thickness, structure, and electrical or superconducting properties. Fig. 5 depicts the variation in T_e with varying working pressures, spanning a range from 0.04 to 0.33 mbar, while maintaining a constant discharge voltage of 600 V. It was observed that the T_e decreases as the working pressure rises. This phenomenon may be attributed to the fact that as the working pressure increases, the density of neutral gas atoms (e.g., nitrogen or argon in the case of NbN deposition) rises. Consequently, electrons in the plasma encounter more frequent collisions with these gas atoms, resulting in a higher collision rate. This increased collision rate leads to electrons losing energy more rapidly, which in turn results in a decrease in electron temperature. In other words, the average energy of electrons in the plasma decreases. Lower T_e at higher pressures can result in a reduction of the deposition rate due to the fact that fewer energetic electrons are available for the ionization of the sputtering gas or precursor materials. Furthermore, this phenomenon can also influence the energy and density of the ionized species arriving at the substrate, which in turn affects the quality and properties of the deposited film, including adhesion and density. In contrast the increase in plasma density with rising working pressure during the deposition of NbN thin layers (as illustrated in Fig. 5), can be attributed to a number of factors pertaining to the behavior of the plasma under conditions of elevated pressure. At higher pressures,

Table 2. A comparison of the experimental (exp.) and standard (std.) values of interplanar spacing (d_{hkl}) for NbN peaks, based on varying Ar:N_2 gas ratios, obtained from XRD data

Ar:N_2 ratios	Phase	2θ, °	FWHM, °	d_{hkl} exp., nm	Grain size, nm	d_{hkl} std. nm	hkl	Crystalline system
80:20	NbN	22.9	0.25	0.38804	32.4	0.380	(200)	cubic
70:30	NbN	23.15	0.55	0.37986	14.8	0.342	(200)	cubic

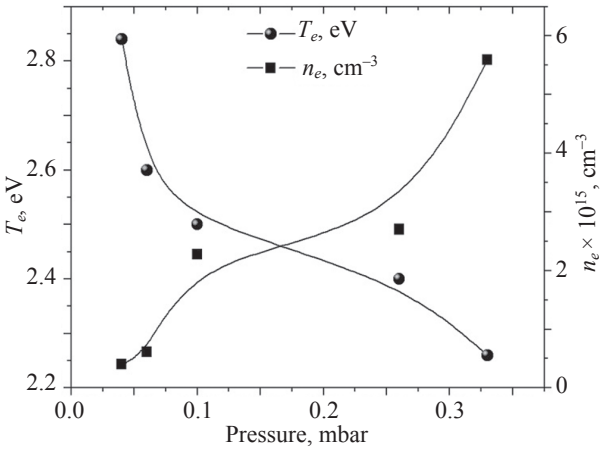

Fig. 5. Electron temperature and density as a function of operational pressures

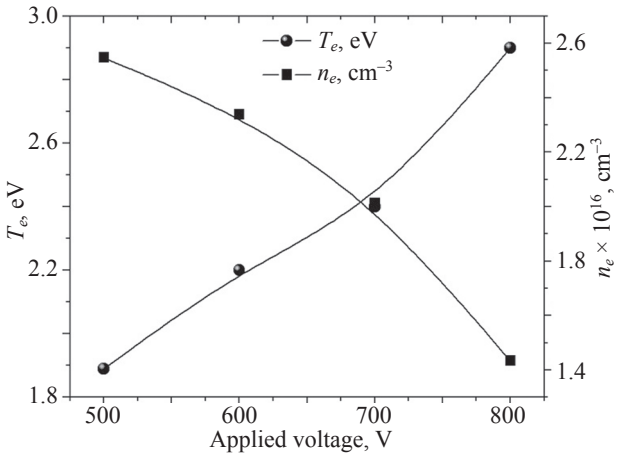

Fig. 6. Electron temperature and density as a function of applied voltage

the density of neutral gas atoms increases, leading to more frequent collisions between electrons and neutral species. Even though the T_e decreases (as mentioned earlier), the overall collisional frequency goes up, and this increases the likelihood of ionization events. In particular, more frequent collisions mean that even electrons with lower energy (due to the lower temperature) are more likely to ionize neutral atoms or molecules, resulting in an increase in the number of ions (i.e., higher plasma density) [25]. Understanding and controlling the relationship between working pressure and plasma density is crucial for optimizing the deposition process and achieving high-quality NbN thin layers tailored for specific applications such as in superconducting devices or hard coatings.

Fig. 6 illustrates the effect of discharge voltage on T_e and n_e. The voltage was recorded at a constant pressure of 0.04 mbar, with measurements taken from 500 to 800 V. As the discharge voltage increases, the ne decreases, while the T_e increases. An increase in the applied voltage during the deposition process results in a corresponding rise in the electric field within the plasma. This electric field accelerates the electrons, causing them to gain more kinetic energy. The kinetic energy of electrons in plasma is commonly described by a T_e which reflects the average energy of the electrons. As the applied voltage increases, the energy imparted to the electrons rises, leading to an increase in electron temperature. This higher electron temperature boosts ionization rates, sputtering efficiency, and reactivity, leading to changes in the deposition rate and the properties of the resulting NbN thin film. While this can improve film quality, it also needs to be carefully controlled to avoid unwanted stress, defects, or non-ideal phases in the NbN layer. On other hand, as electron temperature rises, the rate of recombination of ions and electrons may also increase, further decreasing electron density. This can be exacerbated in high-voltage conditions where the average electron energy exceeds the ionization potential of the neutral gas. A reduction in electron density may impact the ionization of precursor gases, which is a pivotal step in the deposition process. A diminished electron density could potentially result in a decline in the reactive species essential for the formation of high-quality NbN films, consequently influencing properties such as stoichiometry and crystalline structure [26].

As illustrated in Table 3, there is a notable decline in both λ_D and N_D. Conversely, the value of W_{pe} increases

Table 3. Variation of Debye length, Debye number and plasma frequency with working pressure

Working presser, mbar	Debye length $\lambda_D \times 10^{-4}$, cm	Debye number $N_D \times 10^4$	Plasma frequency $W_{pe} \times 10^9$, red. s^{-1}
0.04	3.52	7.90	1.02
0.05	2.92	6.29	1.39
0.10	1.51	3.25	2.69
0.26	1.38	2.98	2.93
0.33	0.96	2.07	4.21

Table 4. Variation of Debye length, Debye number and plasma frequency with applied voltage

Applied voltage, V	Debye length $\lambda_D \times 10^{-4}$, cm	Debye number $N_D \times 10^3$	Plasma frequency $W_{pe} \times 10^9$, red. s^{-1}
500	4.50	9.7	8.99
600	4.69	10.1	8.62
700	5.06	10.9	7.94
800	6.01	12.1	6.75

in conjunction with an increase in working pressure. At short distances, an increase in electron density enhances the shielding effect, which corresponds to an increase in electron density with increasing pressure. In order to confront the external potential, smaller Debye lengths are required due to the large charge-to-volume ratio. Conversely, N_D is directly proportional to the cube of λ_D and electron density, therefore N_D decreases with increasing pressure. Additionally, the W_{pe} rises in conjunction with density. Consequently, as pressure rises, the number of molecules within the chamber increases, leading to an uptick in both electron density and W_{pe} [27]. The variations in Debye length, Debye number, and plasma frequency as functions of pressure and applied voltage are presented in Tables 3 and 4.

Conclusion

Optical emission spectroscopy has been used to investigate the plasma properties within a magnetron sputtering system, specifically during the deposition of niobium thin layers under various conditions. The study experimentally examined the characteristics of a glow discharge in an Ar:N_2 gas mixture, varying contribution N_2 mixture to 20, 30, and 70 %. The emission intensity of selected spectral lines was analyzed to evaluate the electron temperature and electron number density under differencing operational pressures and applied voltage conditions, while keeping other parameters constant. The results indicate that an N_2 contribution of approximately 30 % in the Ar:N_2 mixture is optimal for the growth of homogeneous nanoparticle coatings compare to the 20 % and 50 % cases. The plasma produced exhibited more complex emission spectra, with enhanced contributions from the vibrational and rotational states of nitrogen, resulting in more pronounced argon lines than those observed when argon was the sole component. Furthermore, an increase in the applied voltage results in a rise in electron temperature, whereas an increase in working pressure is accompanied by a decrease in electron temperature. While the density of electrons decreased with increasing applied voltage, it increased with rising working pressure. The temperature of electron to range between 1.8 and 2.9 eV and the electron density was found to be about of 10^{15} to 10^{16} cm^{-3}.

References

1. Laroussi M. Low temperature plasma jets: characterization and biomedical. *Plasma*, 2020, vol. 3, no. 2, pp. 54–58. https://doi.org/10.3390/plasma3020006
2. Hankins O.E., Bourham M.A., Mann D. Observations of visible light emission from interactions between an electrothermal plasma and a propellant. *IEEE Transactions on Magnetics*, 1997, vol. 33, no. 1, pp. 295–298. https://doi.org/10.1109/20.559972
3. Pereira S., Pinto E., Ribeiro P.A., Sério S. Study of a Cold Atmospheric Pressure Plasma jet device for indirect treatment of squamous cell carcinoma. *Clinical Plasma Medicine*, 2019, vol. 13, pp. 9–14. https://doi.org/10.1016/j.cpme.2018.09.001
4. Roomy H., Yasoob N., Murbat H. Evaluate the argon plasma jet parameters by optical emission spectroscopy. *Kuwait Journal of Science*, 2023, vol. 50, no. 2, pp. 163–167. https://doi.org/10.1016/j.kjs.2023.03.001
5. Lars Z. Overview of electric field applications in energy and process engineering. *Energies*, 2018, vol. 11, no. 6, pp. 1361. https://doi.org/10.3390/en11061361
6. Jabur Y.K., Hammed M.G., Khalaf M.K. DC glow discharge plasma characteristics in Ar/O_2 gas mixture. *Iraqi Journal of Science*, 2021, vol. 62, no. 2, pp. 475–482. https://doi.org/10.24996/ijs.2021.62.2.13
7. Jabur Y.K., Khalaf M.K., Hammed M.G. A comparative study of the electrical characteristics of generating argon plasma in different inter-electrode spacing discharges. *International Journal of Nanoelectronics and Materials*, 2020, vol. 13, no. 3, pp. 493–500.
8. Zaplotnik Z., Primc G., Vesel A. Optical emission spectroscopy as a diagnostic tool for characterization of atmospheric plasma jets. *Applied Sciences*, 2021, vol. 11, no. 5, pp. 2275. https://doi.org/10.3390/app11052275
9. Hameed T.A., Kadhem S.J. Plasma diagnostic of gliding arc discharge at atmospheric pressure. *Iraqi Journal of Science*, 2019, vol. 60, no. 12, pp. 2649–2655. https://doi.org/10.24996/ijs.2019.60.12.14
10. Wybranowski T., Ziomkowska B., Cyrankiewicz M., Bosek M., Pyskir J., Napiórkowska M., Kruszewski S. A study of the oxidative processes in human plasma by time-resolved fluorescence spectroscopy. *Scientific Reports*, 2022, vol. 12, no. 1, pp. 9012. https://doi.org/10.1038/s41598-022-13109-0
11. Stryczewska H.D., Boiko O. Applications of plasma produced with electrical discharges in gases for agriculture and biomedicine. *Applied Sciences*, 2022, vol. 12, no. 9, pp. 4405. https://doi.org/10.3390/app12094405
12. Dyatko N.A., Ionikh Y.Z., Napartovich A.P. Influence of nitrogen admixture on plasma characteristics in a DC argon glow discharge and in afterglow. *Atoms*, 2019, vol. 7, no. 1, pp. 13. https://doi.org/10.3390/atoms7010013

Литература

1. Laroussi M. Low temperature plasma jets: characterization and biomedical // Plasma. 2020. V. 3. N 2. P. 54–58. https://doi.org/10.3390/plasma3020006
2. Hankins O.E., Bourham M.A., Mann D. Observations of visible light emission from interactions between an electrothermal plasma and a propellant // IEEE Transactions on Magnetics. 1997. V. 33. N 1. P. 295–298. https://doi.org/10.1109/20.559972
3. Pereira S., Pinto E., Ribeiro P.A., Sério S. Study of a Cold Atmospheric Pressure Plasma jet device for indirect treatment of squamous cell carcinoma // Clinical Plasma Medicine. 2019. V. 13. P. 9–14. https://doi.org/10.1016/j.cpme.2018.09.001
4. Roomy H., Yasoob N., Murbat H. Evaluate the argon plasma jet parameters by optical emission spectroscopy // Kuwait Journal of Science. 2023. V. 50. N 2. P. 163–167. https://doi.org/10.1016/j.kjs.2023.03.001
5. Lars Z. Overview of electric field applications in energy and process engineering // Energies. 2018. V. 11. N 6. P. 1361. https://doi.org/10.3390/en11061361
6. Jabur Y.K., Hammed M.G., Khalaf M.K. DC glow discharge plasma characteristics in Ar/O2 gas mixture // Iraqi Journal of Science. 2021. V. 62. N 2. P. 475–482. https://doi.org/10.24996/ijs.2021.62.2.13
7. Jabur Y.K., Khalaf M.K., Hammed M.G. A comparative study of the electrical characteristics of generating argon plasma in different inter-electrode spacing discharges // International Journal of Nanoelectronics and Materials. 2020. V. 13. N 3. P. 493–500.
8. Zaplotnik Z., Primc G., Vesel A. Optical emission spectroscopy as a diagnostic tool for characterization of atmospheric plasma jets // Applied Sciences. 2021. V. 11. N 5. P. 2275. https://doi.org/10.3390/app11052275
9. Hameed T.A., Kadhem S.J. Plasma diagnostic of gliding arc discharge at atmospheric pressure // Iraqi Journal of Science. 2019. V. 60. N 12. P. 2649–2655. https://doi.org/10.24996/ijs.2019.60.12.14
10. Wybranowski T., Ziomkowska B., Cyrankiewicz M., Bosek M., Pyskir J., Napiórkowska M., Kruszewski S. A study of the oxidative processes in human plasma by time-resolved fluorescence spectroscopy // Scientific Reports. 2022. V. 12. N 1 P. 9012. https://doi.org/10.1038/s41598-022-13109-0
11. Stryczewska H.D., Boiko O. Applications of plasma produced with electrical discharges in gases for agriculture and biomedicine // Applied Sciences. 2022. V. 12. N 9. P. 4405. https://doi.org/10.3390/app12094405
12. Dyatko N.A., Ionikh Y.Z., Napartovich A.P. Influence of nitrogen admixture on plasma characteristics in a DC argon glow discharge and in afterglow // Atoms. 2019. V. 7. N 1. P. 13. https://doi.org/10.3390/atoms7010013

13. Wu Y., Cheng J.-H., Sun D.-W. Blocking and degradation of aflatoxins by cold plasma treatments: Applications and mechanisms. *Trends in Food Science & Technology*, 2021, vol. 109, pp. 647–661. https://doi.org/10.1016/j.tifs.2021.01.053
14. Ananthanarasimhan J., Gangwar R.K., Leelesh P., Srikar P.S.N.S.R., Shivapuji A.M., Roa L. Estimation of electron density and temperature in an argon rotating gliding arc using optical and electrical measurements. *Journal of Applied Physics*, 2021, vol. 129, no. 22, pp. 223301. https://doi.org/10.1063/5.0044014
15. Carter J.A., Barros A.I., Nóbrega J.A., Donati G.L. Traditional calibration methods in atomic spectrometry and new calibration strategies for inductively coupled plasma mass spectrometry. *Frontiers in Chemistry*, 2018, vol. 6, pp. 504. https://doi.org/10.3389/fchem.2018.00504
16. Higuchi T., Noma M., Yamashita M., Urabe K., Hasegawa S., Eriguchi. K. Characterization of surface modification mechanisms for boron nitride films under plasma exposure. *Surface and Coatings Technology*, 2019, vol. 377, pp. 124854. https://doi.org/10.1016/j.surfcoat.2019.07.071
17. Nasakina E.O., Sevostyanov M.A., Baikin A.S., Konushkin S.V., Sergienko K.V., Kaplan M.A., Fedyuk I.M., Leonov A.V., Kolmakov A.G. Using of magnetron sputtering for biocompatible composites creating. *Advances in Composite Materials Development*, 2018, pp. 3–23. https://doi.org/10.5772/intechopen.79609
18. Doyle S.J. *A study of optical and physical probe diagnostic techniques for atmospheric-pressure plasmas*. A thesis degree of Master of Science in Engineering. Huntsville, University of Alabama, 2017. 109 p.
19. Adams S.F., Murray C.S., Pohl N.A. Electron temperature measurement from neutral atomic tungsten emission line ratio. *Review of Scientific Instruments*, 2025, vol. 96, no. 1, pp. 013502. https://doi.org/10.1063/5.0238579
20. Khalaf M.K., Al-Gaffer A.N.A., Mohsin R.H. Estimation of plasma parameters in vanadium magnetron sputtering using optical emission spectroscopy at different experimental formation conditions. *AIP Conference Proceedings*, 2020, vol. 2290, pp. 050040. https://doi.org/10.1063/5.0027435
21. Devia D.M., Rodriguez-Restrepo L.V., Restrepo-Parra E. Methods employed in optical Emission Spectroscopy Analysis: a review. *Ingeniería y Ciencia*, 2015, vol. 11, no. 21, pp. 239–267. https://doi.org/10.17230/ingciencia.11.21.12
22. Ley H. Analytical methods in plasma diagnostic by optical emission spectroscopy: a tutorial review. *Journal of Science and Technology*, 2014, vol. 6, no. 1, pp. 49–66.
23. Bittencourt J.A. *Fundamentals of Plasma Physics*. Springer, 2004, 679 p. https://doi.org/10.1007/978-1-4757-4030-1
24. Dobbyn K. *Design and application of a plasma impedance monitor for RF plasma diagnostics*. A thesis for the degree of Master of Science. Dublin City University, 2000. 84 p.
25. Akatsuka H., Tanaka Y. Discussion on electron temperature of gas-discharge plasma with non-Maxwellian electron energy distribution function based on entropy and statistical physics. *Entropy*, 2023, vol. 25, no. 2, pp. 276. https://doi.org/10.3390/e25020276
26. Chen H., Yuan D., Wu A., Lin X., Li X. Review of low-temperature plasma nitrogen fixation technology. Waste Disposal & Sustainable *Energy*, 2021, vol. 3, no. 3, pp. 201–217. https://doi.org/10.1007/s42768-021-00074-z
27. Goldston R.J., Rutherford P.H. *Introduction to Plasma Physics*. CRC Press, 1995, 510 p. https://doi.org/10.1201/9780367806958

13. Wu Y., Cheng J.-H., Sun D.-W. Blocking and degradation of aflatoxins by cold plasma treatments: Applications and mechanisms // Trends in Food Science & Technology. 2021. V. 109. P. 647–661. https://doi.org/10.1016/j.tifs.2021.01.053
14. Ananthanarasimhan J., Gangwar R.K., Leelesh P., Srikar P.S.N.S.R., Shivapuji A.M., Roa L. Estimation of electron density and temperature in an argon rotating gliding arc using optical and electrical measurements // Journal of Applied Physics. 2021. V. 129. N 22. P. 223301. https://doi.org/10.1063/5.0044014
15. Carter J.A., Barros A.I., Nóbrega J.A., Donati G.L. Traditional calibration methods in atomic spectrometry and new calibration strategies for inductively coupled plasma mass spectrometry // Frontiers in Chemistry. 2018. V. 6. P. 504. https://doi.org/10.3389/fchem.2018.00504
16. Higuchi T., Noma M., Yamashita M., Urabe K., Hasegawa S., Eriguchi. K. Characterization of surface modification mechanisms for boron nitride films under plasma exposure // Surface and Coatings Technology. 2019. V. 377. P. 124854. https://doi.org/10.1016/j.surfcoat.2019.07.071
17. Nasakina E.O., Sevostyanov M.A., Baikin A.S., Konushkin S.V., Sergienko K.V., Kaplan M.A., Fedyuk I.M., Leonov A.V., Kolmakov A.G. Using of magnetron sputtering for biocompatible composites creating // Advances in Composite Materials Development. 2018. P. 3–23. https://doi.org/10.5772/intechopen.79609
18. Doyle S.J. A study of optical and physical probe diagnostic techniques for atmospheric-pressure plasmas. A thesis degree of Master of Science in Engineering. Huntsville, University of Alabama, 2017. 109 p.
19. Adams S.F., Murray C.S., Pohl N.A. Electron temperature measurement from neutral atomic tungsten emission line ratio // Review of Scientific Instruments. 2025. V. 96. N 1. P. 013502. https://doi.org/10.1063/5.0238579
20. Khalaf M.K., Al-Gaffer A.N.A., Mohsin R.H. Estimation of plasma parameters in vanadium magnetron sputtering using optical emission spectroscopy at different experimental formation conditions // AIP Conference Proceedings. 2020. V. 2290. P. 050040. https://doi.org/10.1063/5.0027435
21. Devia D.M., Rodriguez-Restrepo L.V., Restrepo-Parra E. Methods employed in optical Emission Spectroscopy Analysis: a review // Ingeniería y Ciencia. 2015. V. 11. N 21. P. 239–267. https://doi.org/10.17230/ingciencia.11.21.12
22. Ley H. Analytical methods in plasma diagnostic by optical emission spectroscopy: a tutorial review // Journal of Science and Technology. 2014. V. 6. N 1. P. 49–66.
23. Bittencourt J.A. Fundamentals of Plasma Physics. Springer, 2004. 679 p. https://doi.org/10.1007/978-1-4757-4030-1
24. Dobbyn K. Design and application of a plasma impedance monitor for RF plasma diagnostics. A thesis for the degree of Master of Science. Dublin City University, 2000. 84 p.
25. Akatsuka H., Tanaka Y. Discussion on electron temperature of gas-discharge plasma with non-Maxwellian electron energy distribution function based on entropy and statistical physics // Entropy. 2023. V. 25. N 2. P. 276. https://doi.org/10.3390/e25020276
26. Chen H., Yuan D., Wu A., Lin X., Li X. Review of low-temperature plasma nitrogen fixation technology // Waste Disposal & Sustainable Energy. 2021. V. 3. N 3. P. 201–217. https://doi.org/10.1007/s42768-021-00074-z
27. Goldston R.J., Rutherford P.H. Introduction to Plasma Physics. CRC Press, 1995. 510 p. https://doi.org/10.1201/9780367806958

Authors

Harakat Mohsin Roomy — PhD, Full Professor, Ministry of Education, Baghdad, 10011, Iraq, https://orcid.org/0000-0002-7919-4463, hrkatm37@gmail.com
Mohammed K. Khalaf — PhD, Full Professor, Ministry of Science and Technology, Baghdad, 10011, Iraq, https://orcid.org/0000-0001-5688-6304, mohammed.k.khalaf@src.edu.iq
Mohammed G. Hammed — PhD, Full Professor, University of Anbar, Anbar, 31011, Iraq, SC 59162014200, https://orcid.org/0000-0002-0226-702X, Sc.moh72_gh@uoanbar.edu.iq

Авторы

Руми Мохсин Харакат — PhD, профессор, профессор, Министерство образования, Багдад, Ирак, https://orcid.org/0000-0002-7919-4463, hrkatm37@gmail.com
Халаф К. Мохаммед — PhD, профессор, профессор, Министерство образования, Багдад, Ирак, https://orcid.org/0000-0001-5688-6304, mohammed.k.khalaf@src.edu.iq
Хаммед Г. Мохаммед — PhD, профессор, профессор, Университет Анбар, колледж науки, Анбар, 31011, Ирак, SC 59162014200, https://orcid.org/0000-0002-0226-702X, Sc.moh72_gh@uoanbar.edu.iq

Received 12.02.2025
Approved after reviewing 12.06.2025
Accepted 19.07.2025

Статья поступила в редакцию 12.02.2025
Одобрена после рецензирования 12.06.2025
Принята к печати 19.07.2025